# Supplementary Materials for the paper

# Effect of multivalent cations on intermolecular association of isotactic and atactic poly(methacrylic acid) chains in aqueous solutions

**Patricija Hriberšek [1] and Ksenija Kogej [1,*]**

[1] Department of Chemistry and Biochemistry, Faculty of Chemistry and Chemical Technology, University of Ljubljana, SI-1000 Ljubljana, Slovenia; patricija.hribersek@fkkt.uni-lj.si; ksenija.kogej@fkkt.uni-lj.si

* Correspondence: ksenija.kogej@fkkt.uni-lj.si; Tel.: +386-1-479-8538

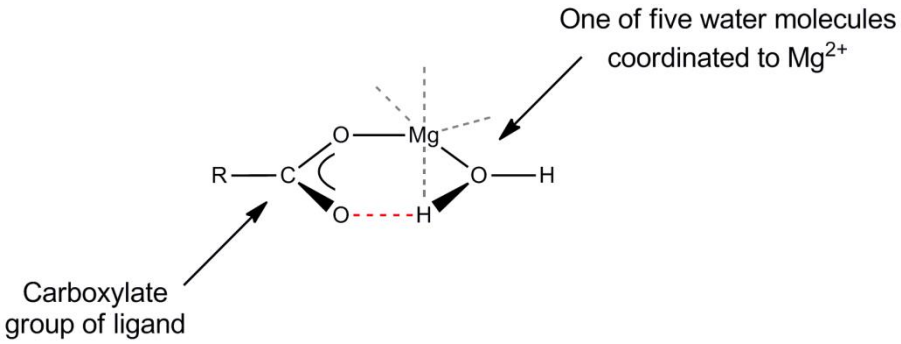


**Scheme S1.** Schematic presentation of monodentate binding of $COO^-$ to $Mg^{2+}$. Presented are the $COO^-$ group, one of the five water molecules coordinated to $Mg^{2+}$ (the position of the other four is indicated with grey dashed lines), and favourable hydrogen-bonding (red dashed bond) interaction between this water molecule and metal-free oxygen of $COO^-$.

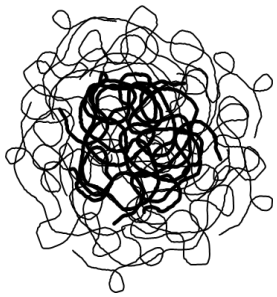

**Scheme S2.** A typical structure of a microgel-like particle with a compact core, impermeable for the solvent, and a swollen outer corona that allows the solvent to penetrate through. aPMA forms particles with less compact cores, while iPMA associates have denser core due to hydrogen bonding between COOH groups.

**Materials and Methods**

*Light scattering.* Methodological aspects of dynamic (DLS) and static (SLS) light scattering can be found elsewhere [1,2,3]. Detailed aspects of data analysis used in this paper are also presented in previous publications [4,5]. Below we shortly give the approach used in our manuscript.

Correlation functions of intensity of scattered light ($G_2(t)$) were recorded at an angle $\theta$ simultaneously with the integral time averaged intensities ($I_\theta \equiv I_q$, where $q = (4\pi n_o/\lambda_o)\sin(\theta/2)$ is the scattering vector, $n_o$ is the refractive index of the medium and $\lambda_o$ is the wavelength of the incident light). Intensities measured in counts of photons per second (cps) were normalized with respect to the Rayleigh ratio of toluene thus converting the cps-units into absolute intensity units given in $cm^{-1}$. In order to determine the hydrodynamic radii of particles, $G_2(t)$ was converted into the correlation function of the scattered electric field ($g_1(t)$) by using the Siegert's relationship [1,2]:

$$g_2(t) = 1 + \beta|g_1(t)|^2$$

or

$$|g_1(t)| = \beta^{-\frac{1}{2}}\sqrt{\frac{G_2(t)}{G_2(\infty)} - 1}$$

where $G_2(\infty)$ is the experimentally determined baseline, $g_2(t) = G_2(t)/G_2(\infty)$, and $\beta$ is the coherence factor determined by the geometry of the detection. Usually it is between $0.5 \le \beta \le 0.8$. The $g_1(t)$ function was analyzed by CONTIN analysis in order to determine distributions of the hydrodynamic radii ($R_h$) of particles in solutions. Example of such distribution obtained at a fixed $q$ is presented in Figure S1 and was used to estimate the mean hydrodynamic radii of larger particles ($R_{h,ass}$; *c.f.* peak 2 in Figure S1a and peak 3 in Figure S1b) and also to split the total intensity of scattered light into contributions of individual populations. This was described in detail in [6].

a) iPMA

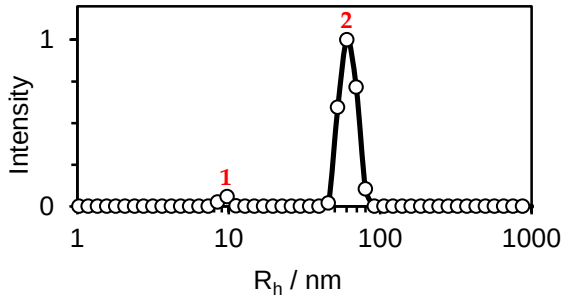


b) aPMA

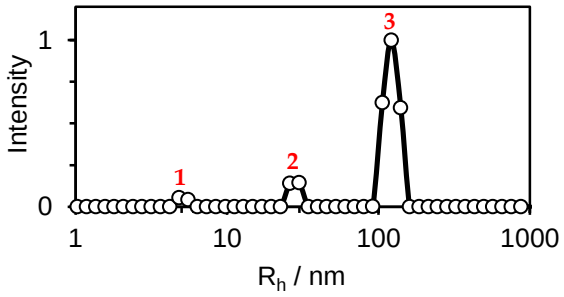


**Figure S1.** The distribution of hydrodynamic radii ($R_h$) of particles obtained in solutions of a) iPMA ($c_P$ = 0.022 mol $L^{-1}$, $\alpha_N$ = 0.19) in 0.0033 M $MgCl_2$ and b) aPMA ($c_P$ = 0.023 mol $L^{-1}$, $\alpha_N$ = 0) in 0.0333 M $MgCl_2$ at $\theta$ = 90°. In the iPMA case, peak 1 corresponds to particles with $R_{h,1}$ and peak 2 to associates with $R_{h,ass}$. In the aPMA case, peaks 1 and 2 correspond to individual chains and possibly smaller associates with $R_{h,1}$ and $R_{h,2}$, respectively, while peak 3 applies to larger aggregates with $R_{h,ass}$.

Hydrodynamic radii of associates ($R_{h,ass}$), which are reported in Tables S1 and S2, were obtained by extrapolation of the $R_{h,app}$ values to $\theta = 0°$ as demonstrated in Figure S2.

$R_h$ of smaller particles and individual chains ($R_{h,1}$ and $R_{h,2}$) reported in Tables S1 and S2 were calculated as the average of $R_h$ values measured at several $q$ values, because they were independent of the angle.

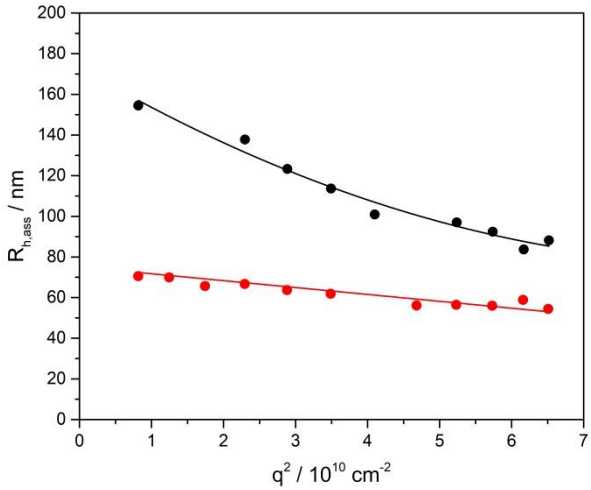


**Figure S2.** Examples of $R_{h,ass}$ determination as extrapolation of $R_h$ values to $\theta = 0°$ for iPMA (red) associates ($c_P$ = 0.022 mol L$^{-1}$, $\alpha_N$ = 0.19) in 0.0033 M $MgCl_2$ and for aPMA (black) associates ($c_P$ = 0.023 mol L$^{-1}$, $\alpha_N$ = 0) in 0.0333 M $MgCl_2$.

From the scattering intensities of the aggregates, the form factor $P(\theta)$ was calculated as $P(\theta) = \frac{I_\theta}{I_0}$. $P(\theta)$ depends on the size and shape of particles and enables the determination of the radius of gyration ($R_g$) [1,2,3].

The Debye-Bueche scattering function [1,2,3] was found to be the most suitable to determine the radius of gyration of larger particles or associates ($R_{g,ass}$) (see an example of the suitable plot in Figure S3):

$$P(\theta) = \frac{1}{(1 + \frac{(qR_g)^2}{6})^2}.$$

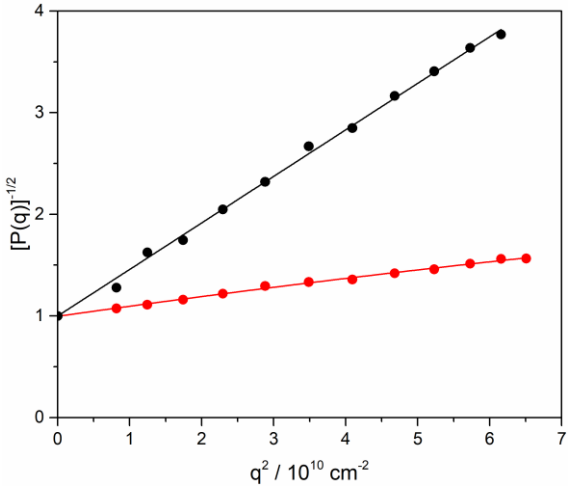


**Figure S3.** Examples of the Debye-Bueche plots ($1/\sqrt{\mathbf{P(\theta)}}$ vs. $q^2$) for $R_{g,ass}$ determination for iPMA associates (red points; $c_P$ = 0.022 mol L$^{-1}$, $\alpha_N$ = 0.19) in 0.0033 M $MgCl_2$ and for aPMA (black) associates (black points; $c_P$ = 0.023 mol L$^{-1}$, $\alpha_N$ = 0) in 0.0333 M $MgCl_2$.

**Results**

*Calorimetry*. As can be seen from Figure S4 ($\Delta H_{ion} = f(\alpha_N)$) for aPMA in 0.0333 M $MgCl_2$ heat effects are rather large (from around 10 to around 30 kJ $mol^{-1}$) while for aPMA in 0.0167 M $LaCl_3$ they are even higher (up to around 40 kJ $mol^{-1}$). These values are considerably higher than those for solutions of both PMAs with a ten-times lower $I$ (*c.f.* Figure 1 in the main paper). Polyacids eventually precipitated from these solutions. iPMA in 0.0167 M $LaCl_3$ precipitated after a few addition of the titrant (NaOH) and consequently only a few initial $\Delta H_{ion}$ values could be measured at this $I$.

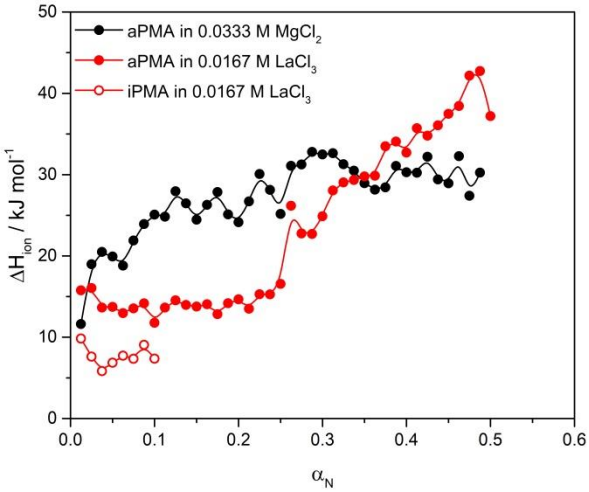


**Figure S4.** Heat effects ($\Delta H_{ion}$ versus $\alpha_N$ curves) measured with ITC during ionization of iPMA and aPMA ($c_P$ = 0.01 mol $L^{-1}$) in solutions of $MgCl_2$ and $LaCl_3$ with $I$ = 0.1 mol $L^{-1}$: aPMA in 0.0333 M $MgCl_2$ and in 0.0167 M $LaCl_3$, and iPMA in 0.0167 M $LaCl_3$.

*Light scattering*.

**Table S1.** Hydrodynamic radii for smaller particles ($R_{h,1}$) and associates ($R_{h,ass}$), radii of gyration ($R_{g,ass}$) and parameter $\rho$ in iPMA solutions ($c_P$ = 0.022 mol $L^{-1}$, different $\alpha_N$) in the presence of NaCl, $MgCl_2$ and $LaCl_3$ at different $I$ at 25 °C.

| Added salt | $I$ / mol $L^{-1}$ | $\alpha_N$ | $R_{h,1}$ / nm | $R_{h,ass}$ / nm | $R_{g,ass}$ / nm | $\rho$ |
|---|---|---|---|---|---|---|
| NaCl | 0.01 | 0.19 | 8 | 59 | / | / |
| | 0.02 | 0.19 | 10 | 80 | 57 | 0.71 |
| $MgCl_2$ | 0.01 | 0.19 | 10 | 75 | 73 | 0.97 |
| $LaCl_3$ | 0.005 | 0.22 | 16 | 191 | 132 | 0.69 |

**Table S2.** Hydrodynamic radii for smaller particles ($R_{h,1}$, $R_{h,2}$) and associates ($R_{h,ass}$), radii of gyration ($R_{g,ass}$) and parameter ϱ in aPMA solutions ($c_P$ = 0.023 mol $L^{-1}$, $\alpha_N$ = 0) in the presence of NaCl, $MgCl_2$ and $LaCl_3$ at different $I$ at 25 °C.

| Added salt | $I$ / mol $L^{-1}$ | $R_{h,1}$ / nm | $R_{h,2}$ / nm | $R_{h,ass}$ / nm | $R_{g,ass}$ / nm | $\rho$ |
|---|---|---|---|---|---|---|
| NaCl | 0.1 | / | 15 | 172 | 126 | 0.73 |
| | 0.2 | / | 13 | 177 | 131 | 0.74 |
| $MgCl_2$ | 0.1 | 6 | 18 | 178 | 164 | 0.92 |
| $LaCl_3$ | 0.05 | 6 | 12 | 183 | 142 | 0.77 |
| | 0.1 | 9 | 15 | 200 | 152 | 0.76 |

*pH measurements*.

**Table S3.** The measured pH and calculated $\alpha_i$ values for iPMA (different $\alpha_N$) and aPMA ($\alpha_N$ = 0) in aqueous NaCl, $MgCl_2$ and $LaCl_3$ with different $I$.

| iPMA | | | | | aPMA | | | |
|---|---|---|---|---|---|---|---|---|
| Added salt | I / mol $L^{-1}$ | $\alpha_N$ | pH | $\alpha_i$ | Added salt | I / mol $L^{-1}$ | pH | $\alpha_i$ |
| / | / | 0.19 | 5.820 | 0.190 | / | / | 3.56 | 0.012 |
| NaCl | 0.01 | 0.19 | 5.840 | 0.190 | NaCl | 0.1 | 3.31 | 0.021 |
| | 0.02 | 0.19 | 5.770 | 0.190 | | 0.2 | 3.28 | 0.023 |
| | | | | | | 0.3 | 3.24 | 0.025 |
| | | | | | | 0.4 | 3.2 | 0.027 |
| | | | | | | 0.5 | 3.17 | 0.029 |
| $MgCl_2$ | 0.01 | 0.19 | 5.680 | 0.190 | $MgCl_2$ | 0.1 | 3.52 | 0.013 |
| | | | | | | 0.2 | 3.45 | 0.015 |
| | | | | | | 0.3 | 3.42 | 0.016 |
| | | | | | | 0.4 | 3.42 | 0.016 |
| | | | | | | 0.5 | 3.44 | 0.016 |
| / | / | 0.22 | 5.980 | 0.220 | $LaCl_3$ | 0.05 | 3.14 | 0.031 |
| $LaCl_3$ | 0.005 | 0.22 | 5.560 | 0.220 | | 0.1 | 3.02 | 0.041 |
| | | | | | | 0.2 | 2.91 | 0.053 |
| | | | | | | 0.3 | 2.87 | 0.058 |
| | | | | | | 0.4 | 2.82 | 0.066 |
| | | | | | | 0.5 | 2.77 | 0.072 |

**References**


[1] Schärtl, W. *Light Scattering from Polymer Solutions and Nanoparticle Dispersions*; Springer Verlag: Berlin, Heidelberg, 2007.

[2] Brown, W. *Dynamic Light Scattering: The Method and Some Application*; Clarendon Press: Oxford, 1993.

[3] Kratochvil, P. Particle scattering functions. In *Particle scattering functions in light scattering from polymer solutions;* Huglin M.B. Ed.; Academic Press Inc.*:* London and New York, 1972; pp. 333−384.

[4] Sitar, S.; Aseyev, V.; Kogej, K. Differences in association behaviour of isotactic and atactic poly(methacrylic acid). *Polymer* **2014**, *55*, 848–854.

[5] Sitar, S.; Aseyev, V.; Kogej, K. Microgel-like aggregates of isotactic and atactic poly(methacrylic acid) chains in aqueous alkali chloride solutions as evidenced by light scattering. *Soft Matter* **2014**, *10*, 7712–7722.

[6] Tarassova, E.V.; Aseyev, V.; Filippov, A.; Tenhu, H. Structure of poly(vinyl pyrrolidone) – $C_{70}$ complexes in aqueous solutions. *Polymer* **2007**, *48*, 4503-4510.